Australian Meteorological and Oceanographic Journal 62 (2012) 25–33

Biomass-burning aerosol over northern Australia

Majed Radhi[1], Michael A. Box[1], Gail P. Box[1] and Ross M. Mitchell[2]
[1]School of Physics, University of New South Wales, Sydney, Australia
[2]CSIRO Marine and Atmospheric Research, Canberra, Australia

(Manuscript received: November 2011; revised April 2012)

Australia's two main continental aerosol types are mineral dust from the arid interior, and smoke from biomass burning in the tropical north. In this study we examine the seasonal cycle of aerosol optical properties from two sites in the Australian tropics: Lake Argyle and Jabiru. In each case we see a distinct seasonal cycle, with highest values of aerosol loading occurring during spring, the height of the savanna burning season. The seasonal cycle of Ångström exponent, a simple but effective guide to particle size, shows that it is fine mode particles which dominate during this time, as expected of biomass burning aerosol. We have also examined size distribution retrievals, and found similar results. An examination of these distributions for successive days showed results consistent with the dual effects of advection, and particle growth expected of smoke aging.

Introduction

Fossil fuel and biomass burning are major sources of anthropogenic aerosol, with degradation of air quality and acid deposition linked to these sources. Smoke from biomass burning could be an important player in cooling the planet by scattering solar radiation. Global-mean direct radiative forcing due to smoke from biomass burning is –0.3 Wm^{-2} (Hobbs et al. 1997). There have been a number of estimates of instantaneous net radiative forcing for heavy biomass-burning aerosol: –36 Wm^{-2} over South America (Christopher et al. 1996); –50 Wm^{-2} at the top of atmosphere and –172 Wm^{-2} at the surface over Canberra (southeast Australia) after a week of bushfires (Mitchell et al. 2006).

Biomass-burning aerosol may exert an indirect radiative forcing through changing cloud microphysics, resulting in an increase of cloud albedo (Twomey et al. 1984; Kaufman and Fraser 1997). In addition biomass-burning aerosol affects air quality and thus has direct health effects (Luhar et al. 2008).

Several studies have estimated the global scale emissions from biomass burning (Seiler and Crutzen 1980; Andreae 1991). Ito and Penner (2004) estimated the total emission from biomass burning to be 2290 Tg C yr^{-1} and they estimated that Australia ranks second in burned area after sub-Saharan Africa with emissions of 33.9 x 10^6 ha yr^{-1}, making up approximately eight per cent of global carbon emissions due to grassland, woodland and forest burning. Many studies have investigated the trace gas emissions from Australian biomass burning in recent years, including BIBLE (Takegawa et al. 2003; Kondo et al. 2003; Shirai et al. 2003), and satellite observation (Edwards et al. 2006).

Shirai et al. (2003) estimated the total Australian biomass burned in 1999 was 255 ± 128 Tg, with 112 ± 64 Tg emission of CO. Edwards et al. (2006) calculated the lifetime of biomass-burning aerosols and found it to be 3.8 ± 0.8 days, which can lead to changes in the physical and optical properties of the particles due to aging processes. With that lifetime intercontinental transport of this aerosol is likely (Rosen et al. 2000).

The processes involved in aging are condensation and coagulation. Condensation involves the addition of volatile compounds to existing particles, resulting in an increase in mass and the growth in size of most particles. This will be reflected in an increase in optical depth, and possibly a minor shift in its spectral dependence. By contrast, coagulation involves the collisional combining of smaller particles to form a smaller number of larger (accumulation mode) particles, without any increase in mass. This is also likely to lead to an increase in optical depth, as the resulting larger particles will now be closer to the radius range of high mass extinction efficiency. In addition, the spectral dependence will clearly be changed at the short wavelength end. Such changes in fine mode particle radius can occur with timescales varying from hours to days (Reid et al. 1998; Radhi et al. 2009). Coagulation is more likely when smoke concentrations are higher.

Australia's tropical north experiences a distinct wet and dry seasonal cycle, and during much of the dry season

Corresponding author address: Dr Michael Box, School of Physics, University of New South Wales, Sydney, NSW, Australia 2052
email: M.Box@unsw.edu.au

(particularly June to November) the savanna is highly susceptible to fire, which is often widespread at this time, producing significant quantities of biomass-burning aerosol. In this study we investigate the daily and monthly variation of aerosol optical thickness, Ångström exponent and size distribution at two sites in northern Australia (Lake Argyle and Jabiru). Previous studies of this aerosol include Bouya et al. (2010) and Bouya and Box (2011), who studied these optical properties in Darwin, for both morning and afternoon (in order to note any sea breeze effects), and Radhi et al. (2006) who examined similar data for Tennant Creek (on the southern edge of the burning zone, ~750 km south of Jabiru).

Study area and data sources

Site locations and dates

Lake Argyle and Jabiru (Fig. 1) are both in the tropical north of Australia. The climate of this region is characterized by hot, humid, wet summers (the monsoon season runs from December to March) and a dry season for much of the rest of the year. The region is covered by dense grass, scattered trees and grassy woodland, and is a source of biomass-burning aerosol due to savanna burning between June and November. The other major aerosol sources in the region are sea salt (when winds are onshore) and mineral dust from the arid interior (Radhi et al. 2006; 2010a).

Fig. 1 Map of Australia showing the location of several AGSNet observing stations, and indicating different aerosol source regions. Seasonal biomass burning occurs in the tropical savanna in the north, evident as the green coloured region that includes the Lake Argyle and Jabiru stations considered here. Dust generation is widespread in the central arid regions, but is particularly prevalent in the Lake Eyre Basin, within which the AGSNet stations at Tinga Tingana and Birdsville are located.

The Lake Argyle station (16.108°S, 128.749°E, 150 m asl) is in a region of longstanding pastoral activity, primarily cattle grazing. The lake itself is the largest freshwater reservoir on the continent and supports irrigation agriculture. The Jabiru station (12.661°S, 132.893°E, 30 m asl) is located in Kakadu National Park approximately 60 km from the coast and is close to the site of the Ranger uranium mine. Our data cover the period 4 April 2002 to 21 December 2005 for Lake Argyle; and 7 December 2001 to 2 May 2006 for Jabiru.

Aerosol optical properties

A multiwavelength solar radiometer measures direct sunlight which has been attenuated on its passage through the atmosphere according to Beer's law, which may be written:

$$I(\lambda) = I_0(\lambda)\exp(-m\tau(\lambda)) \quad \ldots (1)$$

where I is the measured intensity at wavelength λ, I_0 is the intensity outside the atmosphere, m is the airmass factor ($m \approx \sec\theta$, where θ is the solar zenith angle), and τ is the optical thickness, which has components due to Rayleigh (molecular) scattering, gaseous absorption, and aerosol extinction (scattering plus absorption):

$$\tau = \tau_R + \tau_g + \tau_a \quad \ldots (2)$$

Aerosol optical thickness (at a set of wavelengths) is related to the aerosol columnar size distribution via the equation:

$$\tau_a(\lambda) = \int \sigma(r, \lambda) n(r) dr \quad \ldots (3)$$

where σ is the extinction cross section (which also depends on particle refractive index). This is a Fredholm integral equation, and its inversion to obtain the size distribution is a classic ill-posed problem. Nevertheless, a wide range of methods has been developed to extract at least some useful information on the aerosol size distribution.

The simplest approach is to fit a straight line to a log-log plot of τ_a vs λ, using the Ångström expression (valid as a first approximation only):

$$\tau_a(\lambda) \approx \beta\lambda^{-\alpha} \quad \ldots (4)$$

where α is known as the Ångström exponent. Large values of α are generally indicative of smaller particles, and vice versa. A quadratic version of Eqn (3) may sometimes be used to extract additional information (Bouya and Box 2011).

Data sources

All the column Aerosol Optical Thickness (AOT) data used in this study were measured by Cimel Sun photometers which form part of CSIRO's Aerosol Ground Station Network (AGSNet) which is affiliated with NASA's Aerosol Robotic Network (AERONET). Instrument calibration and the

generation of AOT and aerosol microphysical data (phase function, size distribution, refractive index, and derivative quantities such as single scattering albedo and asymmetry factor) were performed as part of the standard AERONET processing stream. These instruments and data products are described in detail by Holben et al. (1998), and Dubovik and King (2000), respectively. Nevertheless, a short description will be given here.

The instrument makes direct sun measurements and sky scans automatically with a 1.2° full field of view at least every fifteen minutes at the nominal wavelengths of 340, 380, 440, 500, 675, 870, 940 and 1020 nm. A full measurement set, including three solar intensity measurements at each wavelength, takes one to two minutes. These measurements are used to compute aerosol optical thickness at each wavelength apart from the 940 nm channel, which is used to retrieve water vapour. Eck et al. (1999) found that the uncertainties in computed AOT are in the range 0.01–0.02 for field instruments. The AOT data are cloud screened following the methodology of Smirnov et al. (2000). The temporal variability of AOT measurements is the principal filter used for cloud screening. Note that we extracted the Ångström exponent over a wavelength range of 440 to 870 nm.

The size distributions have been obtained from version 2 of the AERONET retrieval software. The research and development of this inversion are described by Dubovik and King (2000) and Dubovik et al. (2000). By combining spectral extinction measurements with scattered light measurements (almucantar and principal plane), these instruments are capable of providing information on coarse mode particles as well as accumulation mode. Spherical and non-spherical aerosol particles are assumed in the retrievals (Dubovik et al. 2006). Dubovik et al. (2000) estimate the error in the retrieved distribution is not less than one tenth of its maximum value.

Related observations

No regular monitoring of aerosol chemistry is undertaken in this region. However, the Australian Defence Science and Technology Organisation (DSTO), in conjunction with CSIRO, undertook twin campaigns in the vicinity of Jabiru during June and September of 2003 (Carr et al. 2005), involving both ground-based and airborne sampling and analysis. This is the dry season, so that biomass-burning aerosol was expected to dominate (and was their primary focus). Here we present a brief summary of their findings, which will be useful in the interpretation of our results in the next section.

Ground-based sampling was done using a MOUDI sampler (nine sets), with samples analysed using both Ion Beam Analysis and Ion Chromatography: similar to the procedures employed by Radhi et al. (2010a). Total carbon, organic carbon, and apparent elemental carbon were also evaluated by thermal-optical transmission. Airborne measurements were not as detailed as the ground-based sampling, but were largely consistent with them.

As the focus of this study was biomass-burning aerosol, the detailed results presented were for the fine mode: PM1 ('particulate matter with diameter less than 1 μm'). Mineral dust and sea salt are mostly coarse mode. (Magnesium, a marker for sea salt, was predominantly found in the coarse fraction, for example.) Species that might be expected in biomass-burning aerosol were predominant in the fine fraction, with higher concentrations in September than June. The coarse mode had a typical modal diameter of around 3μm, and its major component appeared to be sea salt (plus a soil component). This was enhanced in September when overnight winds were from the northwest (i.e. onshore).

Qin and Mitchell (2009) have examined ground-based radiometer data to identify the major episodic aerosol types over Australia. They restricted their data set to cases where AOT_{440} exceeded 0.2 (4559 records), both to ensure data reliability, and to isolate events where one aerosol type was likely to dominate. They then used cluster analysis, and found four aerosol types, which they identified as aged smoke, fresh smoke, coarse dust, and a super-absorptive class of unknown type, and have extracted representative size distributions, as well as optical properties at four wavelengths. (They did not identify a sea salt class, most likely as a result of the AOT cut-off.) At Jabiru, these classes were found to occur with frequencies of 56 per cent, 30 per cent, 4 per cent and 7 per cent, respectively, while at Lake Argyle they occurred with frequencies of 38 per cent, 46 per cent, 8 per cent and 5 per cent.

Results

Daily and monthly data

Daily and monthly means of AOT_{500} (AOT at 500 nm) for both sites are presented in Fig. 2. From the graphs it is clear that there is a seasonal cycle in AOT_{500} over these sites with minimum values following the conclusion of the wet season in April, and maximum values during the dry season peaking in October. It is also evident that the daily mean shows large fluctuations during the biomass burning season; approximately 90 per cent of the daily average values have a standard deviation less that 0.05 but this reduces to around 80 per cent during the biomass burning season. (The fluctuation in daily mean at Jabiru during the wet season is most likely due to local sea salt advection.)

The monthly mean of AOT_{500} over these sites increases through the late dry season, peaking in October, as a result of savanna burning at that time of the year. The maximum monthly mean AOT_{500} for Lake Argyle and Jabiru is 0.30 and 0.33 respectively. The annual means computed from monthly means are 0.117 ± 0.078 and 0.159 ± 0.084 for Lake Argyle and Jabiru respectively.

It is clear from the pattern of monthly mean values of Ångström exponent, α, in Fig. 3, that three periods of differing aerosol type can be identified for both sites. The first, from December to March (the wet season), is characterized by low values of α, implying coarse mode particles (likely to

be either sea salt or mineral dust); the second, from April to July (the early dry season), shows the growing influence of fine mode particles as the value of α increases; the third from August to November (the late dry season), characterized by high values of α, is when fine mode particles dominate.

This seasonality in both AOT_{500} and α is what would be expected from the meteorology, and the biomass burning regime, and is consistent with the results of Bouya et al. (2010) for Darwin, and Radhi et al. (2006) for Tennant Creek, who found similar seasonal cycles in their data.

Seasonal statistics

Seasonal frequency distributions of daily mean values of AOT_{500} and α for these sites are presented in Fig. 4 and seasonal averages are given in Table 1. The seasonal breakdown used here—DJFM (wet season); AMJJ (early dry season); ASON (late dry season)—is more appropriate to the tropics than traditional mid-latitude seasons, and is consistent with the conclusions drawn from Fig. 3. The graphs show different patterns for each season, reflecting the different amounts and types of aerosol in the atmosphere. Figure 5 shows seasonal scatter plots of α against AOT_{500} for each site. Such plots may show that large values of AOT_{500} are associated with large or small values of α, and hence are most likely the result of an influx of a certain aerosol type.

The DJFM AOT_{500} frequency patterns are reasonably broad with a clearly defined peak. The Lake Argyle peak occurs at 0.09 and the Jabiru peak at 0.15. These differences are reflected in the daily means with Lake Argyle having the lower seasonal mean (0.11) and Jabiru the higher (0.17). The higher mean for Jabiru is a reflection of its closer proximity to the coast, and hence to sea salt advection. The α histograms are broad and relatively flat, and concentrated in the range indicative of larger particles.

The DJFM α vs. AOT_{500} scatter plot for Jabiru shows a weak trend of α values decreasing as AOT_{500} values increase, which indicates that coarse mode particles, possibly sea salt or mineral dust, are the main contribution to the larger aerosol optical thickness days during this season. For Lake Argyle there is no clear pattern (apart from two data points), which indicates no aerosol type dominated. Being further from the coast, Lake Argyle is less likely to be noticeably affected by sea salt. However, it should be noted that Radhi et al. (2011) found significant sea salt levels in one of their

Fig. 2 Daily and monthly mean values of AOT_{500}.

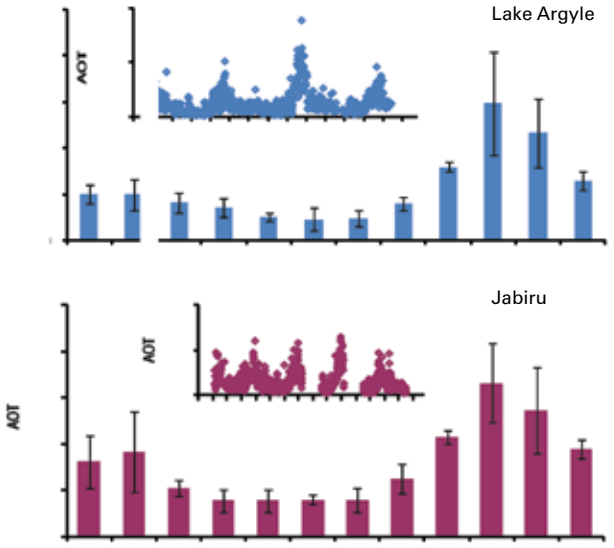

Fig. 3 Monthly mean values of α.

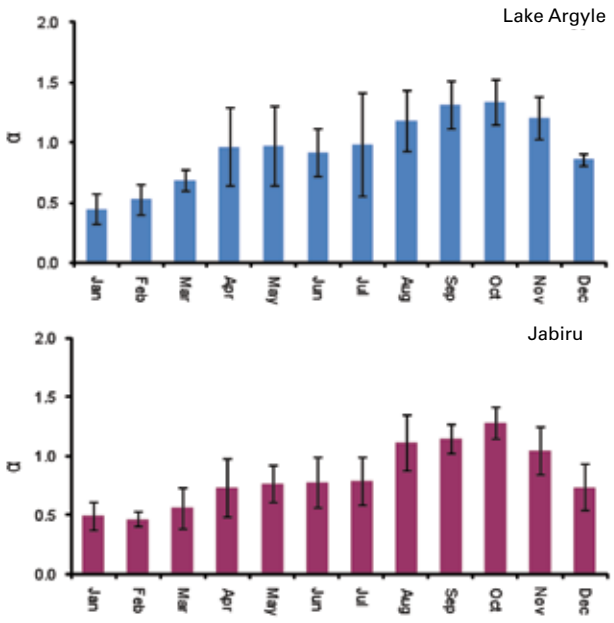

Fig. 4. Seasonal frequency distributions (wet [top]; early dry [middle]; late dry [bottom]) of daily means of AOT_{500} and α.

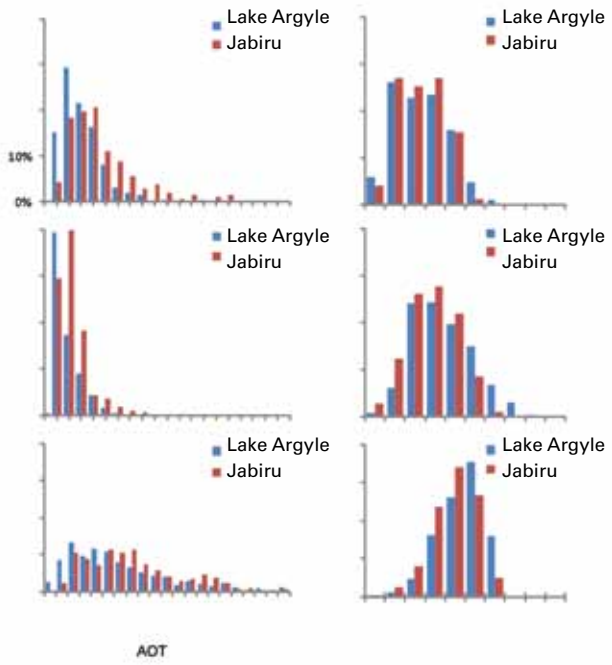

Table 1. Seasonal statistics of AOT and α.

	AOT_{500}				α			
	Lake Argyle		*Jabiru*		*Lake Argyle*		*Jabiru*	
Season	*Mean*	*SD*	*Mean*	*SD*	*Mean*	*SD*	*Mean*	*SD*
DJFM	0.104	0.052	0.152	0.082	0.653	0.406	0.626	0.346
AMJJ	0.054	0.035	0.082	0.042	0.985	0.447	0.795	0.368
ASON	0.195	0.137	0.228	0.124	1.259	0.331	1.123	0.327

samples at Fowlers Gap, roughly ten times as far from the sea as Lake Argyle, when the winds were favourable.

During AMJJ the AOT_{500} frequency distributions were narrow for both sites and the 0.06–0.12 bins accounted for 85 per cent or more of the observations. The seasonal means were lower than for the wet season (Table 1) at both sites. The α histograms for both sites were broad and relatively flat, hinting at a normal distribution. Taking the 0.4 bin as an indicator for coarse particles and the 1.6 bin for fine particles it can be seen that there is a decrease in the fraction of α values in the 0.4 bin and an increase in the 1.6 bin compared to DJFM for both sites. This shift towards higher α values is reflected in the higher seasonal averages for this period (Table 1).

Figure 5 (AMJJ) shows hints of a 'banana' trend for Lake Argyle, where an increase in AOT_{500} was accompanied by both high and low values of α, indicating two different types of aerosol entered the atmosphere. The Jabiru data is less clear. During the early dry season (May–June), fire management officers initiate burns in the still-wet vegetation to avoid large and potentially dangerous fires in the late dry season (September–November). This suggests that the high α days are due to biomass burning. The low α days may be the result of sea salt (Carr et al. 2005), or dust when the wind direction is appropriate.

Fig. 5 Seasonal scatter plots of daily mean of α against AOT_{500}.

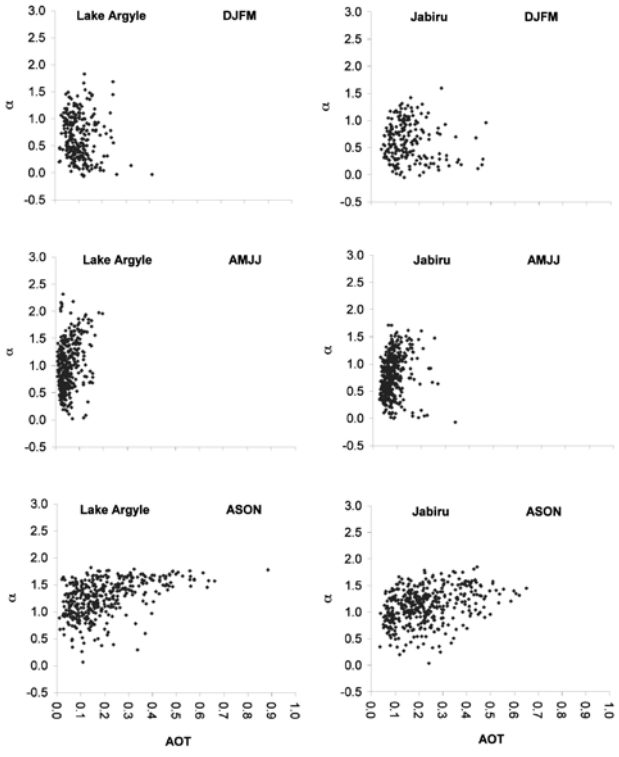

During ASON the AOT_{500} patterns at both sites were broad with peaks at much higher values than the early dry season, with a long tail and a significant proportion of values greater than 0.3. The seasonal mean increased rapidly for both sites by contrast with the other seasons, which indicates high aerosol loading in the northern Australian atmosphere at this time of the year due to biomass burning. The α distribution was negatively skewed for both sites with strong peaks at $1.3 < \alpha < 1.6$. The seasonal means for this period were the highest, which is consistent with an increased proportion of fine particles.

Figure 5 (ASON) shows that the α values were in the 1.2 – 1.8 range for AOT_{500} greater than 0.2 for both sites which indicates that fine mode particles are the major contributor to the high aerosol optical thickness days during this season. It is clear from the above discussion that during the late dry season biomass-burning aerosol contributed significantly to the aerosol optical thickness, and especially so on high AOT_{500} days, which is what would be expected, as biomass burning is very active in the north of Australia during much of the dry season. These results are consistent with Bouya et al. (2010) for Darwin, and Radhi et al. (2006) for Tennant Creek, who found similar seasonality in their data, and also with Carr et al. (2005), who found more biomass-burning aerosol at Jabiru in September than in June.

Size distributions

Daily mean aerosol volume size distributions obtained from AERONET were used to calculate monthly mean volume size distributions over the Lake Argyle and Jabiru sites and are presented in Fig. 6. All show the bimodal character typical of AERONET retrievals. They are also consistent with the size distributions obtained by Qin and Mitchell (2009) for their smoke and dust classes (based on AERONET retrievals).

The Lake Argyle plots show that during the wet season the coarse mode dominates the distribution with the peak at radii in the 5.0 to 6.5 μm range. During the early dry season (April–August) bimodal distributions with the minimum aerosol concentrations were observed. The influence of biomass burning on the distribution is clear during the late

dry season (September–November) as the fine mode peak is dominant. During this season this peak occurred at 0.11 µm radius, which is slightly smaller than the accumulation mode radius for Zambian smoke (r = 0.17 µm) (Eck et al. 2003) and Brazilian smoke (r = 0.13 µm) (Remer et al. 1998). The coarse mode peak during this season was broad with most values in the range 1.7–5 µm and a mode radius 4–5 µm. While this could be due to windblown dust, or sea salt, Qin and Mitchell's (2009) smoke size distributions do contain a small coarse mode.

The Jabiru plots show maximum aerosol concentrations and bimodal distributions during spring (SON) and are broadly similar to the Lake Argyle distributions. The September accumulation mode peaked at 0.11 µm in radius while for October and November it was in the range 0.11–0.15 µm which may be a result of aging processes as the biomass-burning aerosol level builds up, increasing coagulation rates. Of the spring months, the accumulation mode concentration was lowest in September, higher during October, while during November it shows a slight decrease reflecting the variations in the monthly mean AOT. The coarse mode during the spring months was broad with a mode radius around 4.0 µm and had a higher magnitude than for the other seasons: this is consistent with the coarse mode observed by Carr et al. (2005).

Temporal variations in aerosol size distribution

Day-to-day changes in aerosol size distribution may be the result of changes in advection (and hence sources), or atmospheric processing. As the smoke level builds over several days aging may occur due to coagulation and condensation (Reid et al. 1998), leading to an increase in the radius of the accumulation mode peak. In order to investigate this process, and the influence of different aerosol types on size distribution, the daily mean volume size distributions during the period 25–29 October 2004 over Lake Argyle were investigated. Back trajectory analysis shows that the wind was advected from different directions during this period. Six 48-hour back trajectories were run for each day, shown in Fig. 8, with a representative starting height of 1000 m (http://ready.arl.noaa.gov/HYSPLIT.php).

Figure 7 shows that on the 25th the mode radius of the accumulation mode was at 0.11 µm, but on the 26th the fine mode peak had shifted to 0.15 µm in radius with lower concentrations in the accumulation mode which may be due to a reduction in the number of particles as a result of aging processes. On the 25th and 26th (not shown), the wind was onshore (Fig. 8), and from the area south of Darwin, recirculating mixed aerosol air masses, which would allow time for smoke coagulation to occur. Some contribution from Southeast Asian biomass-burning aerosol is also possible (Rotstayn et al. 2007).

On the 27th the AOT_{440} increased to 1.07 leading to a rapid increase in the magnitude of accumulation mode concentration at 0.15 µm radius, but this magnitude sharply decreased on the 28th as the AOT_{440} reduced to 0.69 and the coarse mode became broader and shifted towards smaller sizes. On both of these days the winds were from the east (Fig. 8), and had travelled over savanna burning areas of Arnhem Land.

On the 29th as the AOT_{440} increased to 0.75 the accumulation mode peak at 0.11 µm increased significantly in magnitude while the coarse mode was very broad with a peak closer to smaller sizes and with much higher magnitude than for the other days. On this day the air mass was partly from the Lake Eyre Basin, thus the contribution of dust particles to aerosol optical thickness is likely on this day.

The Ångström exponent on these five days was 1.69, 1.74, 1.77, 1.59 and 1.45 respectively. These values can be compared with those of Qin and Mitchell (2009) for their fresh smoke (Table 2). We see that for the first three days

Fig. 6 (a) Monthly mean volume size distributions over Lake Argyle; and (b) Monthly mean volume size distributions over Jabiru.

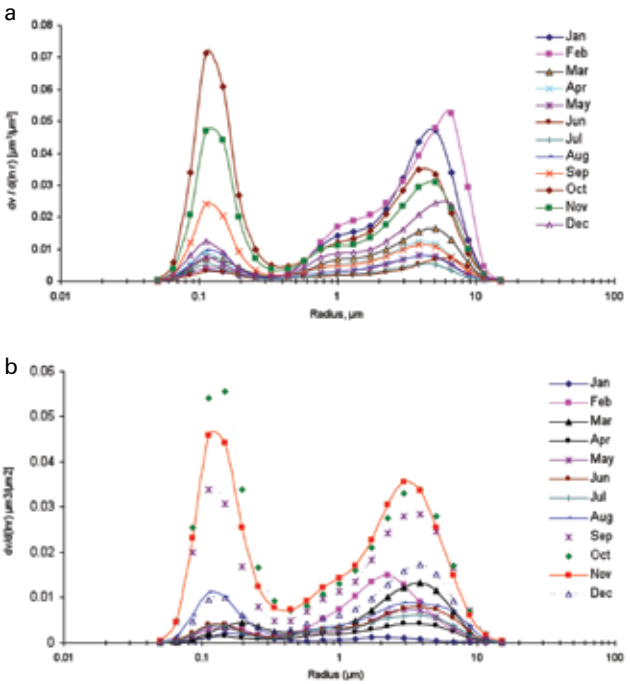

Fig. 7 Daily mean volume size distribution for 25–29 October 2004 over Lake Argyle.

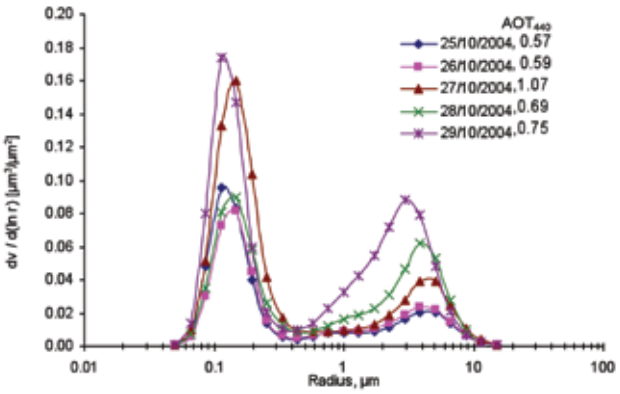

Fig. 8 Air mass back trajectory analysis over Lake Argyle for 25–29 October 2004.

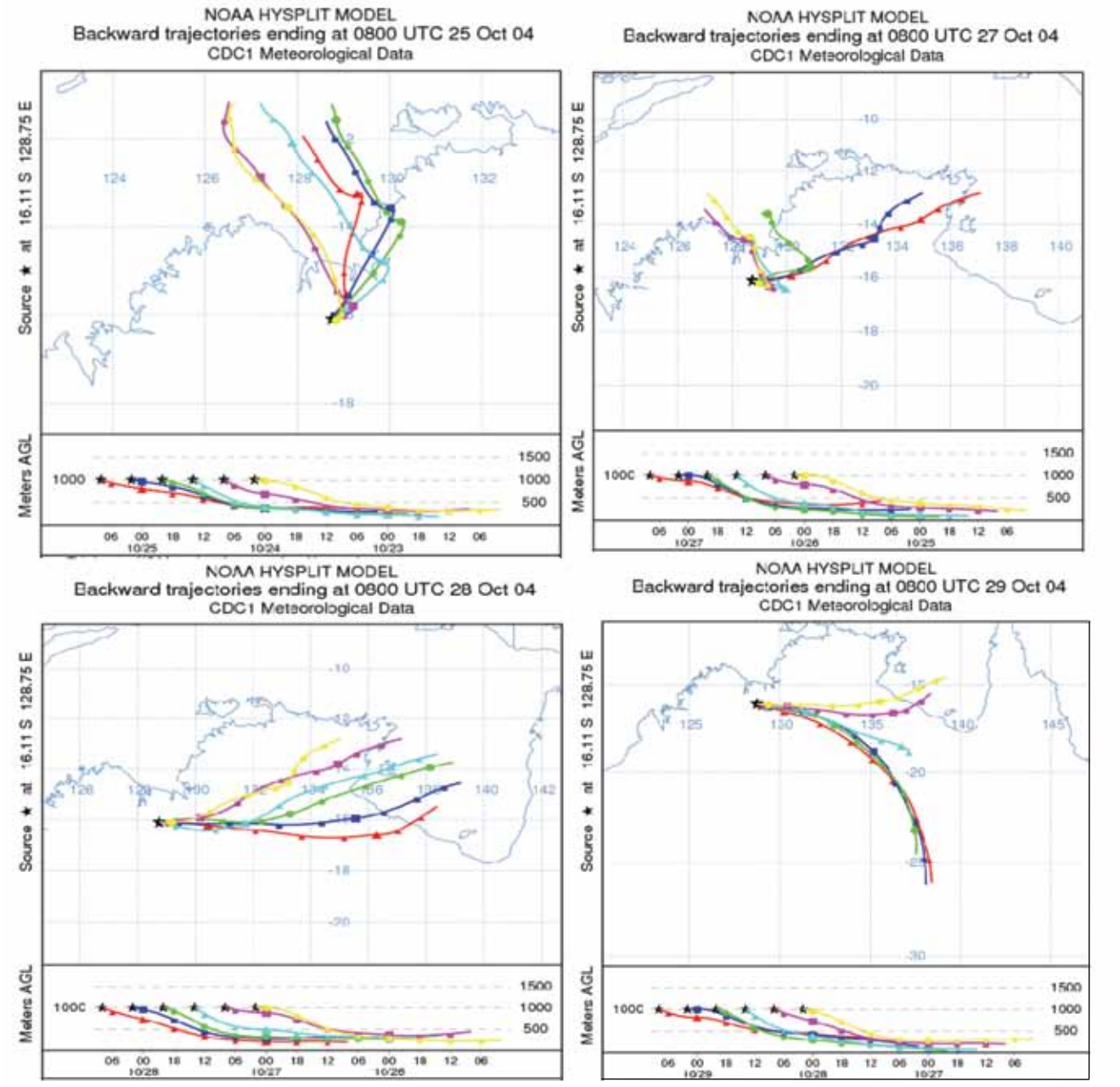

these values are consistent with fresh smoke, but moved towards that of aged smoke on the last two days. From the above discussion it appears likely that both differing sources, and smoke aging processes, made contributions to the changes in aerosol optical properties with time.

Discussion

The Australian atmosphere contains four main aerosol types: mineral (desert) dust; biomass-burning; sea salt; and urban/industrial pollutants. Australia's production of urban/industrial emissions is small by comparison with most industrialised countries, as a result of our low population density and corresponding low intensity of heavy industry. Sydney's monthly mean AOT_{500} is generally less than 0.1 (Box et al. 2002), a low value for any city of its size. Cohen et al. (2011) regularly track the elemental composition of urban aerosol in Sydney, and other Australian cities (Chan et al. 2008), while Gupta et al. (2007) have shown how air quality may be monitored from space.

Australia is the southern hemisphere's major producer of mineral dust, with the majority sourced from the Lake Eyre Basin. Australia's desert area is reddish, in contrast to the yellow of most northern hemisphere deserts. This is a reflection of the higher levels of iron, in the form of hematite,

in the soils (Qin and Mitchell 2009; Radhi et al. 2010a; 2010b; Radhi et al. 2011). Drought conditions during much of the past decade, combined with periodic fluvial resupply of fine sediments, appear responsible for a recent increase in aerosol loading in the Australian interior (Mitchell et al. 2010). Australia also occasionally experiences massive dust storms which transport desert material across the east coast (McTainsh et al. 2005; Radhi et al. 2010c; Jayaratne et al. 2011).

Our studies of Lake Eyre Basin aerosols also revealed the presence of secondary aerosol components such as nitrates and organic acid ions (Radhi et al. 2010a; 2010b; 2011). Sea salt aerosol was present wherever it could be carried by onshore winds, up to ~1000 km, and also methanesulphonic acid, an oxidation product of dimethyl sulphide.

Australia is a naturally dry country, thanks primarily to its latitude, but compounded by the El Niño/La Niña cycle. This makes it extremely vulnerable to fire, particularly in the hotter, northern parts, but also in the southeast (Mitchell et al. 2006; Radhi et al. 2009). Australia's tropics experience a distinct wet and dry seasonal cycle, and during much of the dry season the savanna is highly susceptible to fire, which produces significant quantities of biomass-burning aerosol, the subject of this investigation.

For both Lake Argyle and Jabiru the AOT_{500} graphs show an annual cycle with maximum values during the late dry season, when biomass burning is most active. This seasonality is consistent with studies by Edwards et al. (2006) (satellite observations), Bouya et al. (2010) for Darwin, and Radhi et al. (2006) for Tennant Creek. The α graphs show that during late winter and spring high values occurred, which indicates that fine mode particles dominate. In addition, it is clear from scatter plots of α against AOT_{500} that α values increased as AOT_{500} increased during the late dry season (ASON) at both sites. A quick scan of single scattering albedo data for a selection of these days showed values consistent with smoke aerosols. It is clear from the above results that during late winter and spring the fine fraction contributed strongly to the aerosol optical thickness, and was the primary cause of high AOT_{500} days.

Examination of the monthly average size distribution plots shows that fine mode particles are dominant during the burning season while coarse mode particles are dominant during the wet season, as expected. The identification of an enhanced coarse mode component at both sites during the late dry season calls for further work toward its identification. We also examined a selection of daily size distribution graphs and showed that some of the day-to-day changes are consistent with the changes expected as smoke ages.

References

Andreae, M.O. 1991. Biomass burning: its history, use and distribution, and its impact on environmental quality and global climate. In: J. S. Levine, Editor, *Global Burning: Atmospheric, Climatic and Biospheric Implications*, MIT Press, Cambridge, MA:3–21.

Bouya, Z., Box, G.P. and Box, M.A. 2010. Seasonal variability of aerosol optical properties in Darwin, Australia. *J. Atmos. Sol-Terr. Phys., 72,* 726–39.

Bouya, Z. and Box, G.P. 2011. Seasonal variation of aerosol size distributions in Darwin, Australia. *J. Atmos. Sol-Terr. Phys., 73,* 2022–33.

Box, M.A., Box, G.P., Kay, M.J., Kuzmanoski, M. and Cohen, D. 2002. Physical, chemical and radiative properties of aerosols in Sydney, Australia. *Aust. Meteorol. Mag., 51,* 223–8.

Carr, S.B., Gras, J.L., Hackett, M.T. and Keywood, M.K. 2005. Aerosol characterisation in the Northern Territory of Australia during the dry season with emphasis on biomass burning. DSTO Research Report DSTO-RR-0298, Defence Science and Technology Organisation, Australia.[www.dsto.defence.gov.au/corporate/reports/DSTO-RR-0298.pdf]

Chan, Y.-C., Cohen, D.D., Hawas, O., Stelcer, E., Simpson, R., Denison, L., Wong, N., Hodge, M., Comino, E. and Carswell, S. 2008. Apportionment of sources of fine and course particles in four major Australian cities by positive matrix factorisation. *Atmos. Environ., 42,* 374–89.

Christopher, S.A., Kliche, D.V., Chou, J. and Welch, R.M. 1996. First estimates of the radiative forcing of aerosols generated from biomass burning using satellite data. *J. Geophys. Res., 101,* 21, 265–221, 273.

Cohen, D.D., Stelcer, E., Garton, D. and Crawford, J. 2011. Fine particle characterisation, source apportionment and long-range dust transport into the Sydney Basin: a long term study between 1998 and 2009. *Atmos. Pollution Res., 2,* 182–9.

Dubovik, O. and King, M.D. 2000. A flexible inversion algorithm for retrieval of aerosol optical properties from sun and sky radiance measurements. *J. Geophys. Res., 105,* D16, doi:10.1029/2000JD900282.

Dubovik, O., Smirnov, A., Holben, B. N., King, M. D., Kaufman, Y., Eck, T. F. and Slutsker, I. 2000. Accuracy assessments of aerosol optical properties retrieved from Aerosol Robotic Network (AERONET) sun and sky radiance measurements. *J. Geophys. Res., 105,* D8, doi:10.1029/2000JD900040.

Dubovik, O., Sinyuk, A., Lapyonok, T., Holben, B.N., Mishchenko, M., Yang, P., Eck, T. F., Volten, H., Munoz, O., Veihelmann, B., van der Zande, W.J., Leon, J.-F., Sorokin, M. and Slutsker, I. 2006. Application of spheroid models to account for aerosol particle nonsphericity in remote sensing of desert dust. *J. Geophys. Res., 111,* D11208, doi: 10.1029/2005JD006619.

Eck, T.F., Holben, B.N., Reid, J.S., Dubovic, O., Smirnov, A., O'Neill, N.T., Slutsker, I. and Kinne, S. 1999. Wavelength dependence of the optical depth of biomass burning, urban, and desert dust aerosols. *J. Geophys. Res., 104,* 31, 333–49.

Eck, T.F., Holben, B.N., Ward, D.E., Mukelebai, M.M., Dubovik, O., Smirnov, A., Schafer, J.S., Hsu, N.C., Piketh, S.J., Queface, A., Le Roux, J., Swap, R.P. and Slutsker, I. 2003. Variability of biomass burning aerosol optical characteristics in southern Africa during the SAFARI 2000 dry season campaign and a comparison of single scattering albedo estimates from radiometric measurements. *J. Geophys. Res., 108,* 8477, doi:10.1029/2002JD002321.

Edwards, D.P., Petron, G., Novelli, P.C., Emmons, L.K., Gille, J.C. and Drummond, J.R. 2006. Southern Hemisphere carbon monoxide interannual variability observed by Terra/Measurement of Pollution in the Troposphere (MOPITT). *J. Geophys. Res.. 111,* D16303, doi:16310.11029/12006JD007079.

Gupta, P., Christopher, S.A., Box, M.A. and Box, G.P. 2007. Multi year satellite remote sensing of particulate matter air quality over Sydney, Australia. *Int. J. Rem. Sens., 28,* 4483–4498. doi: 10.1080/01431160701241738.

Hobbs, P.V., Reid, J.S., Kotchenruther, R.A., Ferek, R.J. and Weiss, R. 1997. Direct radiative forcing by smoke from biomass burning. *Science, 275,* 1777–8.

Holben, B.N., Eck, T.F., Slutsker, L., Tanre, D., Buis, J.P., Setzer, A., Vermote, E., Reagan, J.A., Kaufman, Y., Nakajima, T., Lavenu, F., Jankowaif, I. and Smirnov, A. 1998. AERONET – a federated instrument network and data archive for aerosol characterization. *Rem. Sens. Environ., 66,* 1–16.

Ito, A. and Penner, J.E. 2004. Global estimates of biomass burning emissions based on satellite imagery for the year 2000. *J. Geophys. Res., 109,* D14S05, doi:10.1029/2003JD004423.

Jayaratne, E.R., Johnson, G.R., McGarry, P., Cheung, H.C. and Morawska, L. 2011. Characteristics of airborne ultrafine and coarse particles during the Australian dust storm of 23 September 2009. *Atmos. Environ., 45,* 3996–01.

Kaufman, Y.J. and Fraser, R.S. 1997. The effect of smoke particles on clouds and climate forcing. *Science, 277,* 1636–9.

Kondo, Y., Koike, M., Kita, K., Ikeda, H., Takegawa, N., Kawakami, S., Blake, D., Liu, S. C., Ko, M., Miyazaki, Y., Irie, H., Higashi, Y., Liley, B., Nishi, N., Zhao, Y. and Ogawa, T. 2003. Effects of biomass burning, lightning, and convection on O_3, CO, and NO_y over the tropical Pacific and Australia in August–October 1998 and 1999. J. Geophys. Res., 108, 8402, doi:10.1029/2001JD000820.

Luhar, A.K., Mitchell, R.M., Meyer, C.P., Qin, Y., Campbell, S., Gras, J.L. and Parry, D. 2008. Biomass burning emissions over northern Australia constrained by aerosol measurements: II. Model validation, and impacts on air quality and radiative forcing. *Atmos. Environ., 42,* 1647–64.

McTainsh, G., Chan, Y.C. McGowan, H., Leys, J. and Tews, K. 2005. The 23rd October 2002 dust storm in eastern Australia: characteristics and meteorological conditions. *Atmos. Environ., 39,* 1227–36.

Mitchell, R.M., O'Brien, D.M. and Campbell, S.K. 2006. Characteristics and radiative impact of the aerosol generated by the Canberra firestorm of January 2003. *J. Geophys. Res., 111,* D02204, doi:10.01029/02005JD006304.

Mitchell, R.M., Campbell, S.K. and Qin, Y. 2010. Recent increase in aerosol loading over the Australian arid zone. *Atmos. Chem. Phys., 10,* 1689–99.

Qin, Y. and Mitchell, R.M. 2009. Characterisation of episodic aerosol types over the Australian continent. *Atmos. Chem. Phys., 9,* 1943–56.

Radhi, M., Box, M.A., Box, G.P. and Forgan, B.W. 2006. Seasonal cycles of aerosol optical properties at Wagga Wagga and Tennant Creek, Australia. *Clean Air and Environmental Quality, 40(3),* 40–4.

Radhi, M., Box, M.A., Box, G.P., Gupta, P. and Christopher, S.A. 2009. Evolution of the optical properties of biomass-burning aerosol during the 2003 southeast Australian bushfires. *Appl. Opt., 48,* 1764–73.

Radhi, M., Box, M.A., Box, G.P., Mitchell, R.M., Cohen, D.D., Stelcer, E. and Keywood, M.D. 2010a. Optical, physical and chemical characteristics of Australian continental aerosols: results from a field experiment. *Atmos. Chem. Phys., 10,* 5925–42.

Radhi, M., Box, M.A., Box, G.P., Mitchell, R.M., Cohen, D.D., Stelcer, E. and Keywood, M.D. 2010b. Size-resolved mass and chemical properties of dust aerosols from Australia's Lake Eyre Basin. *Atmos. Environ., 44,* 3519–28.

Radhi, M., Box, M.A., Box, G.P. and Cohen, D.D. 2010c. Size-resolved chemical composition of the September 2009 Sydney dust storm. *Air Quality and Climate Change, 44(3),* 25–30.

Radhi, M., Box, M.A., Box, G.P., Keywood, M.D., Cohen, D.D., Stelcer, E. and Mitchell, R.M. 2011. Size-resolved chemical composition of Australian dust aerosol during winter. *Environ. Chem., 8,* 248–62.

Reid, J.S., Hobbs, P.V., Ferek, R.J., Blake, D.R., Martins, J.V., Dunlap, M.R. and Liousse, C. 1998. Physical, chemical, and optical properties of regional hazes dominated by smoke in Brazil. *J. Geophys. Res., 103,* D24, 32,059–80.

Remer, L.A., Kaufman, Y.J., Holben, B.N., Thompson, A.M. and McNamara, D. 1998. Biomass burning aerosol size distribution and modeled optical properties. *J. Geophys. Res., 103,* D24, 31, 879–91.

Rotstayn, L.D., Cai, W., Dix, M.R., Farquhar, G.D., Feng, Y., Ginoux, P., Herzog, M., Ito, A., Penner, J.E., Roderick, M.L. and Wang, M. 2007. Have Australian rainfall and cloudiness increased due to the remote effects of Asian anthropogenic aerosols? *J. Geophys. Res., 112,* D09202, doi:10.1029/2006JD007712.

Rosen, J., Young, S., Laby, J., Kjome, N. and Gras, J. 2000. Springtime aerosol layers in the free troposphere over Australia: Mildura Aerosol Tropospheric Experiment (MATE 98). *J. Geophys. Res., 105,* D14, 17,833–42.

Seiler, W. and, Crutzen P.J. 1980. Estimates of gross and net fluxes of carbon between the biosphere and the atmosphere from biomass burning. *Climatic Change, 2,* 207–47.

Shirai, T., Blake, D.R., Meinardi, S., Rowland, F.S., Russell-Smith, J., Edwards, A., Kondo, Y., Koike, M., Kita, K., Machida, T., Takegawa, N., Nishi, N., Kawakami, S. and Ogawa, T. 2003. Emission estimates of selected volatile organic compounds from tropical savanna burning in northern Australia. *J. Geophys. Res., 108,* D3, 8406, doi:10.1029/2001JD000841.

Smirnov, A., Holben, B.N., Eck, T.F., Dubovik, O. and Slutsker, I. 2000. Cloud-screening and quality control algorithms for the AERONET database. *Remote Sens. Environ., 73,* 337–49.

Takegawa, N., Kondo, Y., Koike, M., Ko, M., Kita, K., Blake, D.R., Nishi, N., Hu, W., Liley, J.B., Kawakami, S., Shirai, T., Miyazaki, Y., Ikeda, H., Russel-Smith, J. and Ogawa, T. 2003. Removal of NO_x and NO_y in biomass burning plumes in the boundary layer over northern Australia. *J. Geophys. Res., 108,* D10, 4308, doi:10.1029/2002JD002505.

Twomey, S.A., Piepgrass, M. and Wolfe, T. L. 1984. An assessment of the impact of pollution on global cloud albedo. *Tellus, 36B,* 356–66.